Received: 1 November 2019 | Revised: 28 January 2020 | Accepted: 22 February 2020

DOI: 10.1002/sim.8528

RESEARCH ARTICLE

Statistics in Medicine WILEY

A phase I-II design based on periodic and continuous monitoring of disease status and the times to toxicity and death

Juhee Lee[1] | **Peter F. Thall**[2] | **Pavlos Msaouel**[3]

[1]Department of Statistics, University of California Santa Cruz, Santa Cruz, California, USA

[2]Department of Biostatistics, The University of Texas MD Anderson Cancer Center, Houston, Texas, USA

[3]Department of Genitourinary Medical Oncology, The University of Texas MD Anderson Cancer Center, Houston, Texas, USA

Correspondence
Juhee Lee, Department of Statistics, University of California Santa Cruz, 1156 High Street Mail Stop SOE2, Santa Cruz, CA 95064 USA.
Email: juheelee@soe.ucsc.edu

Funding information
Conquer Cancer Foundation, Grant/Award Number: Young Investigator Award; Division of Mathematical Sciences, Grant/Award Number: DMS-1662427; Kidney Cancer Association, Grant/Award Number: Young Investigator Award

A Bayesian phase I-II dose-finding design is presented for a clinical trial with four coprimary outcomes that reflect the actual clinical observation process. During a prespecified fixed follow-up period, the times to disease progression, toxicity, and death are monitored continuously, and an ordinal disease status variable, including progressive disease (PD) as one level, is evaluated repeatedly by scheduled imaging. We assume a proportional hazards model with piecewise constant baseline hazard for each continuous variable and a longitudinal multinomial probit model for the ordinal disease status process and include multivariate patient frailties to induce association among the outcomes. A finite partition of the nonfatal outcome combinations during the follow-up period is constructed, and the utility of each set in the partition is elicited. Posterior mean utility is used to optimize each patient's dose, subject to a safety rule excluding doses with an unacceptably high rate of PD, severe toxicity, or death. A simulation study shows that, compared with the proposed design, a simpler design based on commonly used efficacy and toxicity outcomes obtained by combining the four variables described above performs poorly and has substantially smaller probabilities of correctly choosing truly optimal doses and excluding truly unsafe doses.

KEYWORDS

adaptive randomization, Bayesian design, dose finding, interim response, mixed hazard, phase I-II clinical trial

1 | INTRODUCTION

We propose a Bayesian design for a phase I-II clinical trial based on an outcome vector including three time-to-event (TTE) variables and a longitudinal discrete ordinal categorical disease severity process, motivated by a metastatic renal cancer trial. During a fixed follow-up period, the times to progressive disease (PD), toxicity, and death are monitored. Each patient's disease also is evaluated by imaging the tumor at successive scheduled times after the start of treatment. At each evaluation, the possible disease severity levels are PD, stable disease (SD), partial response (PR), and complete response (CR). Thus, PD is monitored in two ways, both as a continuous variable and a discrete variable. Because this structure reflects how patient outcomes actually are observed in many oncology settings, the proposed design is broadly applicable. The design is constructed by first mapping the outcome vector to a finite partition of outcome combinations,

TABLE 1 Utilities of the full outcome design

		$a_T = 1$	$a_T = 2$	$a_T = 3$
		$Y_T \leq 42$	$42 < Y_T \leq 84$	$84 < Y_T$
$a_{PD} = 1$	$Y_{PD} \leq 42$ or $Z_1 = 0$	20	30	45
$a_{PD} = 2$	$42 < Y_{PD} \leq 84$ or $Z_2 = 0$	35	40	50
$a_{PD} = 3$	$84 < Y_{PD}$ and $\boldsymbol{Z} = (1, 1)$	45	50	60
$a_{PD} = 4$	$84 < Y_{PD}$ and $\boldsymbol{Z} = (1, 2)$	50	55	65
$a_{PD} = 5$	$84 < Y_{PD}$ and $\boldsymbol{Z} = (1, 3)$	70	75	85
$a_{PD} = 6$	$84 < Y_{PD}$ and $\boldsymbol{Z} = (2, 1)$	45	50	60
$a_{PD} = 7$	$84 < Y_{PD}$ and $\boldsymbol{Z} = (2, 2)$	60	65	75
$a_{PD} = 8$	$84 < Y_{PD}$ and $\boldsymbol{Z} = (2, 3)$	80	85	95
$a_{PD} = 9$	$84 < Y_{PD}$ and $\boldsymbol{Z} = (3, 1)$	35	40	50
$a_{PD} = 10$	$84 < Y_{PD}$ and $\boldsymbol{Z} = (3, 2)$	35	40	50
$a_{PD} = 11$	$84 < Y_{PD}$ and $\boldsymbol{Z} = (3, 3)$	85	90	100

Note: Elicited utilities $U(\boldsymbol{a})$ of the 33 possible $\boldsymbol{a} = (a_{PD}, a_T, a_D) = (a_{PD}, a_T, 2)$ on the follow-up subintervals (0, 42] and (42, 84] for patients who survive 84 days, that is, $Y_D > 84$ (equivalently, $a_D = 2$). For any $\boldsymbol{a}$ with $a_D = 1$, $U(\boldsymbol{a}) = 0$. For each Z_1 and Z_2, the values (0, 1, 2, 3) represent (PD, SD, PR, CR), so $(a_{PD} = 1 \text{ or } 2) = (Y_{PD} \leq 84)$ and $(a_{PD} \geq 3) = (84 < Y_{PD})$.

based on the disease evaluation schedule and follow-up interval, eliciting a numerical utility for each set in the partition, and using posterior mean utility as a criterion for choosing doses.

The motivating trial aims to optimize the dose of the oral targeted agent sitravatinib, combined with a fixed dose of the immunotherapeutic agent nivolumab, for treating metastatic renal cancer. Nivolumab is a programmed death 1 immune checkpoint inhibitor with proven efficacy against clear cell renal cell carcinoma.[1] Sitravatinib is an oral tyrosine kinase inhibitor that Du et al[2] have shown in preclinical cancer models to potentiate immune checkpoint blockade when combined with drugs such as nivolumab, by targeting cell receptors known to contribute to an immunosuppressive tumor microenvironment. This motivates exploring the combination of nivolumab and sitravatinib clinically in metastatic renal cancer. Tumor imaging is done at 42 and 84 days after the start of treatment using computerized tomography (CT) scan or magnetic resonance imaging (MRI), with disease severity categorized as {CR, PR, SD, PD} using RECIST criteria.[3] Continuous monitoring of the times to toxicity and death is done over 84 days of follow-up, with PD observed continuously as the occurrence time of signs or symptoms that prompt unscheduled imaging that confirms the signs/symptoms occurred due to PD.

Most phase I-II trial designs are based on simplified outcomes defined by combining complex outcomes similar to those described above. This often is done by reducing a sequence of ordinal disease status variables and event time variables to one nominal "efficacy" outcome, and similarly defining one "toxicity" outcome. Defining such simpler outcomes allows an established design to be applied. Phase I-II designs based on binary efficacy and toxicity are given by Braun,[4] Thall and Cook,[5] Yin et al,[6] Mandrekar et al,[7] Yuan and Yin,[8] Thall et al,[9] and Gao and Yuan,[10] and many others. An alternative approach is to define toxicity and efficacy as TTE variables to avoid suspension of patient enrollment, as done, for example, by Yuan and Yin,[11] Thall et al,[12] and Jin et al.[13] Reviews of phase I-II designs have been given by Zohar and Chevret,[14] Yuan et al,[15] and Yan et al.[16]

The convention of defining simplified outcome variables comes with a high price that may not be obvious. While the data reduction may appear sensible to simplify phase I-II modeling and design in this way, because it destroys important information, it may result in a design with surprisingly poor properties. Our simulations, reported below in Section 4, include as a comparator a phase I-II design based on two outcomes, the time to toxicity and "efficacy," defined as neither PD nor death occurring during the 84 days follow-up period. These two outcomes correspond to Case 2 of the phase I-II design of Jin et al,[13] described in sections 2.1 and 5.4 of that paper. Undesirable consequences of using this combined efficacy outcome are illustrated by the following two examples. We first note that both our proposed design based on the full outcome data and the simpler design based on toxicity and the combined efficacy outcome defined above rely on numerical utilities for outcome desirability evaluation, which we will describe in detail below, on a finite number of sets defined in terms of the follow-up subintervals (0, 42] and (42, 84] days. These utilities are given in Table 1 for the full

TABLE 2 Utilities of the reduced outcome design

		$a_T = 1$	$a_T = 2$	$a_T = 3$
		$Y_T \leq 42$	$42 < Y_T \leq 84$	$84 < Y_T$
$a'_{PD} = 1$	$Y'_{PD} \leq 42$	10	20	35
$a'_{PD} = 2$	$42 < Y'_{PD} \leq 84$	25	30	45
$a'_{PD} = 3$	$84 < Y'_{PD}$	60	80	100

Note: Utilities $U'(\boldsymbol{a}')$ of all possible $\boldsymbol{a}$ for the reduced design, based on Y_T and efficacy defined as neither PD nor death occurring by day 84.

outcome design and Table 2 for the reduced outcome design. As a first example, if a patient is alive without PD at day 84 but experiences toxicity before day 42, then the full outcome design may assign this a utility between 45 and 85, depending on the patient's disease statuses at days 42 and 84, while the reduced design's utility is 60 because it ignores different outcome desirabilities implied by ordinal disease status categories, SD, PR, or CR. As a second example, if a patient dies between days 42 and 84, the full outcome design assigns this a utility of 0, whereas the reduced outcome design assigns it a utility of 25, 30, or 45, depending on when toxicity occurs, the same as the event of PD occurrence, although death is a clinically much worse result than PD. An important consequence of the difference between the full outcome design and a design that uses simplified outcomes is that, for their assumed utilities, the two designs may have different truly optimal doses. That is, because simplifying outcomes may easily change the quantification of what is important, the simplified design may have an "optimal" dose that is different from the optimal dose under the design using the full outcome structure. Consequently, computer simulation results of the design based on the simplified outcomes may misleadingly indicate that it has a high probability of choosing the "optimal" dose when consideration of the full outcomes would lead to the conclusion that this dose is suboptimal. Simulations, described below in Section 4.2, show general consequences of this sort of disagreement due to using a design with simplified outcomes. In most scenarios considered, our proposed design based on the full outcome vector is much more likely to choose truly superior doses and protect patient safety, compared with the simpler design.

We assume a Bayesian multivariate semiparametric regression model for the TTE outcomes, $\boldsymbol{Y} = (Y_{PD}, Y_T, Y_D)$, including proportional hazards (PH) models with piecewise constant baseline hazards, and dose effects accounted for by parametric regression. For $\boldsymbol{Z}$, the ordinal categorical variables that represent PD, SD, PR, and CR, we assume a longitudinal multivariate probit regression model, including dose and previous outcomes as covariates. Combining the models for ordinal disease status variables, $\boldsymbol{Z}$, and the continuous time to PD, Y_{PD}, the overall observation process for PD is modeled by a mixture distribution that is discrete at the scheduled imaging times and continuous at the remaining times. Similar to Lee et al,[17] we introduce a random frailty vector for each patient and assume conditional independence of the outcomes given the frailties. The patient-specific frailties account for additional variability between patients not explained by the regression model and induce dependence between the elements of $(\boldsymbol{Y}, \boldsymbol{Z})$. A joint model for $(\boldsymbol{Y}, \boldsymbol{Z})$ is obtained by marginalizing over the frailty vector. Frailty models have been used widely for multivariate failure time data in a wide variety of settings, including competing risks[18] and semicompeting risks.[19] Our proposed design's sequentially adaptive dose selection decisions for patients enrolled during the trial are based on posterior predictive mean utilities, computed from the interim data using elicited numerical utilities of $(\boldsymbol{Y}, \boldsymbol{Z})$ values on partition in the fixed follow-up period.

The remainder of the article is organized as follows. Section 2 presents the probability model underlying the design. Section 3 describes utility elicitation and numerical computation and presents the design. In Section 4, a simulation study is presented to evaluate the design's safety, ability to identify optimal doses, and robustness, and to compare it to a design based on simplified outcomes. We close with a brief discussion in Section 5.

2 | DOSE-OUTCOME MODEL

2.1 | Event times and longitudinal disease status

The disease statuses scored at L scheduled times following the start of therapy are represented as ordinal categorical variables $\boldsymbol{Z} = (Z_1, \ldots, Z_L)$, with each entry Z_ℓ of $\boldsymbol{Z}$ taking on integer values $(0, 1, 2, 3)$ representing (PD, SD, PR, CR). If PD occurs at any evaluation, then, by definition, SD, PR, and CR cannot occur subsequently. The times to severe toxicity and death are denoted by Y_T and Y_D, respectively. We also let Y_{PD} denote the time of PD observed due to the occurrence

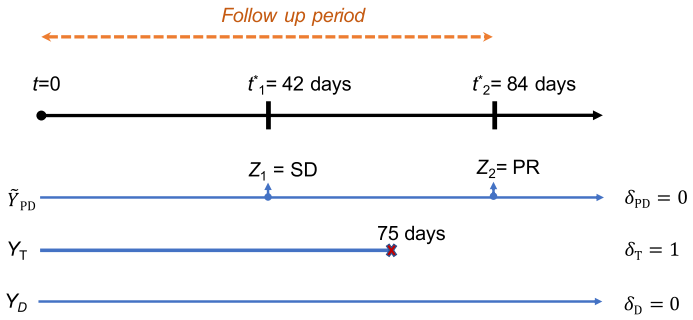

FIGURE 1 Illustration of the observed outcomes $\tilde{\boldsymbol{Y}} = (\tilde{Y}_{\text{PD}}, Y_{\text{T}}, Y_{\text{D}})$ and $\boldsymbol{Z} = (Z_1, Z_2)$. Severe toxicity occurred at day 75, while neither death nor PD occurred during the follow-up period, with imaging conducted at two prespecified times. The outcomes after full follow-up are $\tilde{\boldsymbol{Y}}^o = (84, 75, 84)$, $\boldsymbol{\delta} = (0, 1, 0)$, and $\boldsymbol{Z} = (1, 2)$ [Colour figure can be viewed at wileyonlinelibrary.com]

of signs or symptoms. Occurrence of PD may be observed either by the discrete time imagining process or continuously at time Y_{PD} by signs or symptoms. Since PD may be observed at most once, the definitions of the longitudinal discrete variables $\boldsymbol{Z}$ and the possibly right-censored continuous time variable Y_{PD} are linked. These all are potential outcomes that may or may not be observed during follow-up, and they are semicompeting risks since death censors all other variables at Y_{D}, but not conversely.

For interim sample size $n(t) \leq N_{\max}$ at trial time t in days, index patients in order of enrollment by $i = 1, \ldots, n(t)$, with trial entry times $0 \leq e_1 \leq e_2 \leq \ldots \leq e_{n(t)}$. Given fixed follow-up time C, for patient i, the event $j =$ PD, T, or D occurs at trial time $e_i + Y_{i,j}$, and the three events are monitored continuously until $e_i + C$, subject to possible right-censoring of $e_i + Y_{i,\text{PD}}$ and $e_i + Y_{i,\text{T}}$ by death at $e_i + Y_{i,\text{D}}$. In the renal cancer trial, $C = 84$ days. Each patient's disease status {PD, SD, PR, CR} is evaluated by CT or MRI tumor imaging at follow-up times $e_i + t^\star_{i,\ell}$, $\ell = 1, \ldots, L$, where are $t^\star_{i,1} < \ldots < t^\star_{i,L}$ are prespecified. Denote the ordinal disease status outcome of patient i at time $e_i + t^\star_{i,\ell}$ by $Z_{i,\ell} \in \{0, 1, 2, 3\}$. In general, different ordinal categories may be used to accommodate a particular clinical setting, provided that PD is included. In the renal cancer trial, $L = 2$ and the interim disease evaluation times are $t^\star_{i,1} \in (42 \pm 7)$ and $t^\star_{i,2} \in (84 \pm 7)$, with the ±7-day deviation from each scheduled time included to accommodate commonly seen logistical variability in the process of imaging patients' diseases.

Let $Y^o_{i,j}$ denote the observation time of $Y_{i,j}$ or right-censoring, with binary indicator $\delta_{i,j} = 1$ if $Y^o_{i,j} = Y_{i,j}$ and 0 otherwise. At trial time $t > e_i$, if $Y_{i,\text{D}} > \min\{t - e_i, C\}$, then $Y^o_{i,\text{D}}$ is the time of independent right censoring with $\delta_{i,\text{D}} = 0$, that is, the patient is alive at t. If $Y_{i,\text{D}} < \min\{t - e_i, C\}$, then $Y^o_{i,\text{D}} = Y_{i,\text{D}}$ is the observed time of death, and $\delta_{i,\text{D}} = 1$. The nonfatal outcomes $Y_{i,\text{T}}$, $Y_{i,\text{PD}}$ and $Z_{i,\ell}$, $\ell = 1, \ldots, L$ can be censored administratively at C or by death. For severe toxicity, if $Y_{i,\text{T}} < \min\{t - e_i, C, Y_{i,\text{D}}\}$, then $Y^o_{i,\text{T}} = Y_{i,\text{T}}$ with $\delta_{i,\text{T}} = 1$ and otherwise $Y^o_{i,\text{T}}$ is the time of right-censoring ($\delta_{i,\text{T}} = 0$). Due to the construction, $Y_{i,\text{PD}}$ also may be censored by the event $Z_{i,\ell} = 0$ that PD is seen by imaging. Censoring of $Z_{i,\ell}$ is dependent on $Y_{i,\text{D}}$, $Y_{i,\text{PD}}$, and the events $(Z'_{i,\ell} = 0)$, $\ell' < \ell$. That is, if $Y_{i,\text{PD}}$ or $Y_{i,\text{D}} < t^\star_{i,\ell}$, or $Z_{i,\ell'} = 0$ for $\ell' < \ell$, then $Z_{i,\ell}$ is censored. To connect $\{Z_{i,\ell}\}$ and $Y_{i,\text{PD}}$, we define $\tilde{Y}_{i,\text{PD}}$ to be the time to PD observed by either the continuous variable or by the discrete observation process. Formally,

$$\tilde{Y}_{i,\text{PD}} = \min\{Y_{i,\text{PD}},\ t^\star_{i,\ell} \times 1(Z_{i,\ell} = 0)\} \quad \text{and} \quad \tilde{Y}^o_{i,\text{PD}} = \min\{C, Y_{i,\text{D}}, \tilde{Y}_{i,\text{PD}}\}.$$

If $\tilde{Y}_{i,\text{PD}} = Y_{i,\text{PD}}$ or $Z_{i,\ell} = 0$ for any ℓ, then $\delta_{i,\text{PD}} = 1$; otherwise, let $\delta_{i,\text{PD}} = 0$. An example of $\tilde{\boldsymbol{Y}}^o$, $\boldsymbol{\delta}$ and $\boldsymbol{Z}$ is illustrated in Figure 1. Due to the semi-competing risk structure that death censors any nonfatal event but not conversely, the support of $\tilde{\boldsymbol{Y}}_i = (\tilde{Y}_{i,\text{PD}}, Y_{i,\text{T}}, Y_{i,\text{D}})$ is defined on the set $\mathcal{Y} = \{\tilde{\boldsymbol{y}} \subset [0, \infty)^3 : \max(\tilde{y}_{\text{PD}}, y_{\text{T}}) < y_{\text{D}}\}$.

2.2 | Sampling and frailty models

To develop a dose-outcome model for the coprimary outcome variables $\boldsymbol{Y} = (Y_{\text{PD}}, Y_{\text{T}}, Y_{\text{D}})$, and longitudinal $\boldsymbol{Z}$, we first standardize doses to have mean 0 and variance 1, denoted by $\{d_1, \ldots, d_M\}$. In the renal cancer trial, given the raw doses $(60, 80, 120, 150)$ mg/day of oral sitravatinib, the standardized doses are $(-1.05, -0.56, 0.43, 1.18)$, with $M = 4$. For the ith patient, we denote the assigned dose by $d_{[i]}$ and introduce a frailty vector $\boldsymbol{\gamma}_i = (\gamma_{i,\text{PD}}, \gamma_{i,\text{T}}, \gamma_{i,\text{D}}, \gamma_{i,\text{Z}}) \in \mathbb{R}^4$, where $\gamma_{i,\text{Z}}$ corresponds to $\boldsymbol{Z}_i$. Assuming conditional independence of the outcomes $(\boldsymbol{Y}_i, \boldsymbol{Z}_i)$ given $\boldsymbol{\gamma}_i$, we specify marginal models for $Z_{i,\ell}$ and each $Y_{i,j}$ given $\boldsymbol{\gamma}_i$, and obtain a joint distribution by averaging over the distribution of $\boldsymbol{\gamma}_i$. The joint distribution is identifiable in $\mathcal{Y}$ and the subset of $\mathcal{Z}_\ell(\tilde{Y}_{\text{PD}})$ censored by Y_{D}.[20] We will present a model for $\boldsymbol{\gamma}_i$ below.

We first construct probability models for $Y_{i,\mathrm{PD}}$ and $\boldsymbol{Z}_i = \{Z_{i,\ell}\}$, which together will yield a continuous-discrete mixture model for $\tilde{Y}_{i,\mathrm{PD}}$. For event time $Y_{i,\mathrm{PD}}$ of patient i treated at dose $d_{[i]}$, we assume a PH model with conditional hazard function

$$h_{\mathrm{PD}}(t|d_{[i]}, \boldsymbol{\gamma}_i) = h_{0\mathrm{PD}}(t)\exp\{\eta_{\mathrm{PD}}(d_{[i]}, \boldsymbol{\gamma}_i)\}, \tag{1}$$

where $h_{0\mathrm{PD}}(t)$ is an unknown baseline hazard function, and the function η_{PD} accounts for dose effects on the hazard of Y_{PD}. PD has two observation processes that may be censored at Y_D. This may result in sparse occurrences for each process especially with a small sample size. To obtain a reliable approximation of the occurrence probabilities of PD, we assume a simple model for η_{PD} and use the linear function in the logarithm of the hazard given by $\eta_{\mathrm{PD}}(d_{[i]}, \boldsymbol{\gamma}_i) = \beta_{\mathrm{PD}} d_{[i]} + \gamma_{i,\mathrm{PD}}$, with $\beta_{\mathrm{PD}} \in \mathbb{R}$.

For ordinal disease status $Z_{i,\ell}$ obtained from imaging at $e_i + t^\star_{i,\ell}$, $\ell = 1, \ldots, L$, we assume a multinomial probit model. For simplicity, we will present the model for $L = 2$ scheduled disease evaluations, as in the renal cancer trial. Recall that there are $K = 4$ possible disease states {PD, SD, PR, CR} obtained from each disease imaging. Let $\Phi(\cdot|\mu, \sigma^2)$ denote the cdf of a normal distribution with mean μ and variance σ^2. We introduce a vector of fixed cutoffs $\boldsymbol{u} = (u_0, \ldots, u_K)$ with $u_0 < u_1 < \ldots < u_K$, $u_0 = -\infty$ and $u_K = \infty$. Given $Y_{i,\mathrm{PD}} \geq t^\star_{i,\ell}$ and $Z_{i,\ell'} \neq 0$, $\ell' < \ell$, we apply the common device of using the cutoffs $\boldsymbol{u}$ to define the observed categorical variables $\{Z_{i,\ell}\}$, as in Ashford and Sowden[21] and Chib and Greenberg.[22] Conditioning on $Y_{i,\mathrm{PD}} \geq t^\star_{i,1}$ (equivalently, $\tilde{Y}_{i,\mathrm{PD}} \geq t^\star_{i,1}$), we assume the probit model

$$\begin{aligned} \mathrm{P}(Z_{i,1} = k|d_{[i]}, \boldsymbol{\gamma}_i) &= \pi_{1,k}(d_{[i]}, \boldsymbol{\gamma}_i) \\ &= \Phi(u_{k+1}|\mu_1(d_{[i]}, \boldsymbol{\gamma}_i), \sigma^2_\pi) - \Phi(u_k|\mu_1(d_{[i]}, \boldsymbol{\gamma}_i), \sigma^2_\pi), \end{aligned} \tag{2}$$

with fixed σ^2_π for $k = 0, \ldots, K-1$. The cutoffs $u_1, \ldots, u_{K-1}$ used to define the $Z_{i,\ell}$s are determined from elicited values, as described in Supplement Section 2. Similarly, given that $Y_{i,\mathrm{PD}} \geq t^\star_{i,2}$ and $Z_{i,1} > 0$ (equivalently, $\tilde{Y}_{i,2} \geq t^\star_{i,2}$), we assume

$$\begin{aligned} \mathrm{P}(Z_{i,2} = k|d_{[i]}, Z_{i,1}, \boldsymbol{\gamma}_i) &= \pi_{2,k}(d_{[i]}, Z_{i,1}, \boldsymbol{\gamma}_i) \\ &= \Phi(u_{k+1}|\mu_2(d_{[i]}, Z_{i,1}, \boldsymbol{\gamma}_i), \sigma^2_\pi) - \Phi(u_k|\mu_2(d_{[i]}, Z_{i,1}, \boldsymbol{\gamma}_i), \sigma^2_\pi). \end{aligned} \tag{3}$$

The mean functions in Equations (2) and (3) are given by

$$\mu_1(d_{[i]}, \boldsymbol{\gamma}_i) = \xi_1 + \phi d_{[i]} + \gamma_{i,Z}, \quad \text{and} \quad \mu_2(d_{[i]}, Z_{i,1}, \boldsymbol{\gamma}_i) = \xi_2 + \phi d_{[i]} + \alpha_{Z_{i,1}} + \gamma_{i,Z}. \tag{4}$$

Expression (4) includes imaging time-specific intercepts ξ_1 and ξ_2 for the probit distributions of the ordinal disease status outcomes $Z_{i,1}$ and $Z_{i,2}$ evaluated by imaging, with dose effects accounted for by $\phi \in \mathbb{R}$. The vector $\boldsymbol{\alpha} = (\alpha_1, \ldots, \alpha_{K-1})$ quantifies effects of the first imaged disease status $Z_{i,1}$ on the second imaged disease status $Z_{i,2}$. Since imaging is performed at $t^\star_{i,2}$ only if PD has not occurred prior to $t^\star_{i,2}$, α_0 is not defined. This construction may be extended to settings with $L > 2$ disease imaging in a straightforward manner, although it may be appropriate to make a Markovian assumption by defining $\mu_l(d_{[i]}, Z_{i,1}, \ldots, Z_{i,\ell-1}, \boldsymbol{\gamma}_i)$ as $\mu_l(d_{[i]}, Z_{i,\ell-1}, \boldsymbol{\gamma}_i)$ to control the number of model parameters.

We let $\alpha_1 = 0$ by using $Z_1 = 1$ as the reference and assume $0 < \alpha_2 < \alpha_3$ to reflect the fact that $Z_{i,1}$ is ordinal. Note that the dose-outcome relationship for PD in Equations (1) and (4) is not assumed to be either increasing or decreasing in dose under the model. A multireceptor tyrosine kinase inhibitor, sitravatinib, in our motivating trial is a targeted agent, and there is no strong biological justification to assume monotonicity in one direction rather than another. In contrast to cytotoxic agents, targeted drugs often have different affinities for different receptors, and increasing dose may cause antagonistic biological effects, negative feedback regulation that reduces responses, or receptor desensitization. There also may be dose-dependent modulation of drug metabolism. An overview is given by Lagarde et al.[23] If monotonicity in either direction is known a priori, it can be reflected by restricting the domains of β_{PD} and ϕ appropriately. For mathematical convenience, we use a probit model in Equations (2) and (3). Alternative approaches such as those in Ursino and Gasparini,[24] Piccolo et al,[25] and Wellhagen et al[26] can be considered for defining $Z_{i,\ell}$.

For $\ell = 1, 2$, $[Z_{i,\ell} = 0]$ is the event that PD is observed at $t^\star_{i,\ell}$, and $\pi_{\ell,0}$ is the conditional probability that PD is detected by imaging at time $t^\star_{i,\ell}$ given $\tilde{Y}_{i,\mathrm{PD}} \geq t^\star_{i,\ell}$. This implies that $\pi_{\ell,0}$ is the discrete hazard of PD occurring at $t = t^\star_{i,\ell}$. Similarly, for $k \neq 0$, $\pi_{\ell,k}$ is the conditional probability of observing $Z_{i,\ell} = k$ given $\tilde{Y}_{i,\mathrm{PD}} \geq t^\star_\ell$. Consequently, the hazard function of

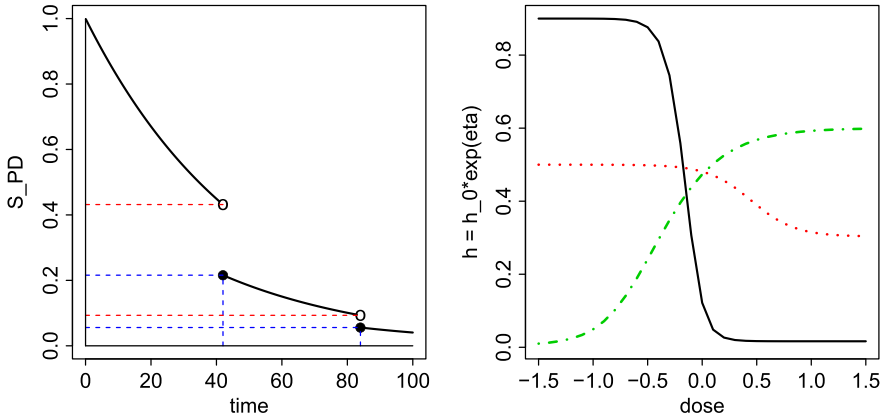

(A) Survival function ($S_{\text{PD}}(t)$) (B) hazard function ($h(t)$)

FIGURE 2 An example of the survival function $S_{\text{PD}}(t)$ with constant hazard h_{PD0} is in (a). The survival functions are discontinuous at $t_1^\star = 42$ and $t_2^\star = 84$. (b) shows an example of the hazard function $h(t)$ with constant baseline hazard h_0 and a logistic function for η. Hazard function $h = h_0 \exp\left\{\frac{\beta_3}{1+\exp(\beta_1(10\times d-\beta_2)}\right\}$. $(\beta_1, \beta_2, \beta_3) = (-1, 0, -4)$, $(-0.5, 5, -0.5)$, and $(0.3, 10, -5)$ with $h_0 = 0.9$, 0.5 and 0.6 are used for the black solid, red dashed, and green dash-dotted lines, respectively [Colour figure can be viewed at wileyonlinelibrary.com]

$\tilde{Y}_{i,\text{PD}}$ is the continuous-discrete mixture

$$h_{\text{PD}}(t|d_{[i]}, \boldsymbol{Z}_i, \boldsymbol{\gamma}_i) = \begin{cases} h_{0\text{PD}}(t)\exp\{\eta_{\text{PD}}(d_{[i]}, \boldsymbol{\gamma}_i)\}, & t > 0,\ t \neq t^\star_{i,\ell}, \quad \ell = 1, 2, \\ \pi_{1,0}(d_{[i]}, \boldsymbol{\gamma}_i), & t = t^\star_{i,1}, \\ \pi_{2,0}(d_{[i]}, Z_{i,1}, \boldsymbol{\gamma}_i), & t = t^\star_{i,2}, \end{cases} \tag{5}$$

where $Z_{i,1} \in \{1, 2, 3\}$ for $\pi_{2,0}$, and the joint survival function of $\tilde{Y}_{i,\text{PD}}$ and $\boldsymbol{Z}_i$ is

$$\text{P}(\tilde{Y}_{i,\text{PD}} > t, \boldsymbol{Z}_i|d_{[i]}, \boldsymbol{\gamma}_i) = \begin{cases} S'_{\text{PD},i}(t), & 0 < t < t^\star_{i,1}, \\ S'_{\text{PD},i}(t)\pi_{1,Z_{i,1}}(d_{[i]}, \boldsymbol{\gamma}_i), & t^\star_{i,1} \le t < t^\star_{i,2}, \\ S'_{\text{PD},i}(t)\pi_{1,Z_{i,1}}(d_{[i]}, \boldsymbol{\gamma}_i)\pi_{2,Z_{i,2}}(d_{[i]}, Z_{i,1}, \boldsymbol{\gamma}_i), & t^\star_{i,2} \le t, \end{cases} \tag{6}$$

where

$$S'_{\text{PD},i}(t) = \exp\left\{-\int_0^t h_{0\text{PD}}(v)\exp\{\eta_{\text{PD}}(d_{[i]}, \boldsymbol{\gamma}_i)\}dv\right\}.$$

Note that the discrete random variables $Z_{i,1}$ and $Z_{i,2}$ appear in the subscripts of the probabilities $\pi_{1,Z_{i,1}}(d_{[i]}, \boldsymbol{\gamma}_i)$ and $\pi_{2,Z_{i,2}}(d_{[i]}, Z_{i,1}, \boldsymbol{\gamma}_i)$, and moreover, the support $\mathcal{Z}_{i,\ell}(t)$ of $Z_{i,\ell}$ changes with t. The mixture survival function $S_{\text{PD}}(t|d_{[i]}, \boldsymbol{\gamma}_i) = \text{P}(\tilde{Y}_{i,\text{PD}} > t|d_{[i]}, \boldsymbol{\gamma}_i)$ is obtained by marginalizing Equation (6) over $\mathcal{Z}_{i,\ell}(t)$. Using the definition of the mixture hazard, the joint distribution of $\tilde{Y}_{i,\text{PD}}$ and $\boldsymbol{Z}_i$ is expressed as

$$\text{P}(\tilde{Y}_{i,\text{PD}} = t, \boldsymbol{Z}_i|d_{[i]}, \boldsymbol{\gamma}_i) = h_{\text{PD}}(t|d_{[i]}, \boldsymbol{Z}_i, \boldsymbol{\gamma}_i)\lim_{v\to t^-}\text{P}(\tilde{Y}_{i,\text{PD}} > v, \boldsymbol{Z}_i|d_{[i]}, \boldsymbol{\gamma}_i), \quad t > 0. \tag{7}$$

An example of $\text{P}(\tilde{Y}_{i,\text{PD}} > t|d_{[i]}, \boldsymbol{\gamma}_i)$ is illustrated in Figure 2A, which shows that the survival function is discontinuous at $t^\star_\ell = 42$ and 84 days due to the discrete components in the hazard function (5).

We formulate probability models for $Y_{i,\text{T}}$ and $Y_{i,\text{D}}$, by assuming PH models similar to Equation (1), with unknown baseline hazard functions $h_{0j}(t)$ and dose-outcome regression functions $\eta_j(d_{[i]}, \boldsymbol{\gamma}_i)$. For $j = T$ and D, we model the relationship between $Y_{i,j}$, d, and $\gamma_{i,j}$ through the regression function

$$\eta_j(d_{[i]}, \boldsymbol{\gamma}_i) = \frac{\beta_{j3}}{1 + \exp\{\beta_{j1} \times (10 \times d_{[i]} - \beta_{j2})\}} + \gamma_{i,j}, \quad \text{for } j = T \text{ and } D, \tag{8}$$

where we assume that $\beta_{j2} \in \mathbb{R}$ and $\beta_{j3} < 0$. We multiply dose by 10 to stabilize computations. The factor 10 was chosen based on preliminary simulation studies. For the dose coefficients, we assume $\beta_{\mathrm{T1}} < 0$ to ensure that η_{T} increases with dose. Since death may be related to severe toxicity or disease progression, let $\beta_{\mathrm{D1}} \in \mathbb{R}$ so the probability of death may increase or decrease in dose. The regression model for Y_{T} and Y_{D} is flexible yet parsimonious. Functions of the form given by Equation (8) commonly are used to obtain an "S" shape, with β_{j2} the inflection point, when allowing nonlinear patterns of a dose effect, such as a plateau in the hazard. An example of h_j with η_j of the form in Equation (8) is illustrated in Figure 2B. The survival functions for the marginal distributions of the times to toxicity and death take the usual forms $S_j(t|d_{[i]}, \boldsymbol{\gamma}_i) = \exp\{-\int_0^t h_j(v|d_{[i]}, \boldsymbol{\gamma}_i)dv\}$, for $j = T, D$.

Let $\boldsymbol{\theta}$ denote the vector of all model parameters and $\tilde{\boldsymbol{\theta}}$ the vector of all fixed hyperparameters, which we will specify below. The joint likelihood of all observable outcomes of patient i, conditional on $d_{[i]}$, $\boldsymbol{\gamma}_i$, and all model parameters, is the product

$$\begin{aligned} p(\tilde{\boldsymbol{y}}_i^o, \boldsymbol{z}_i, \boldsymbol{\delta}_i|d_{[i]}, \boldsymbol{\gamma}_i, \boldsymbol{\theta}, \tilde{\boldsymbol{\theta}}) &= \prod_{j\in\{\mathrm{D,T}\}} p(y_{i,j}^o, \delta_{i,j}|d_{[i]}, \boldsymbol{\gamma}_i, \boldsymbol{\theta}, \tilde{\boldsymbol{\theta}}) \times p(\tilde{y}_{i,\mathrm{PD}}^o, \boldsymbol{z}_i, \delta_{i,\mathrm{PD}}|d_{[i]}, \boldsymbol{\gamma}_i, \boldsymbol{\theta}, \tilde{\boldsymbol{\theta}}) \\ &= \prod_{j\in\{\mathrm{D,T}\}} \left\{ h_{i,j}(y_{i,j}^o|d_{[i]}, \boldsymbol{\gamma}_i) \right\}^{\delta_{i,j}} S_j(y_{i,j}^o|d_{[i]}, \boldsymbol{\gamma}_i) \\ &\quad \times \mathrm{P}(\tilde{y}_{i,\mathrm{PD}}^o, \boldsymbol{z}_i|d_{[i]}, \boldsymbol{\gamma}_i)^{\delta_{i,\mathrm{PD}}}\ \mathrm{P}(\tilde{Y}_{i,\mathrm{PD}} > \tilde{y}_{i,\mathrm{PD}}^o, \boldsymbol{z}_i|d_{[i]}, \boldsymbol{\gamma}_i)^{1-\delta_{i,\mathrm{PD}}}, \end{aligned} \tag{9}$$

where $\tilde{\boldsymbol{y}}_i^o = (y_{i,\mathrm{D}}^o, y_{i,\mathrm{T}}^o, \tilde{y}_{i,\mathrm{PD}}^o)$, $\boldsymbol{z}_i = (z_{i,1}, z_{i,2})$, and $\boldsymbol{\delta}_i = (\delta_{i,\mathrm{D}}, \delta_{i,\mathrm{T}}, \delta_{i,\mathrm{PD}})$.

For the patient frailties, we assume $\boldsymbol{\gamma}_i|\Omega \overset{iid}{\sim} \mathrm{N}_4(\mathbf{0}, \Omega)$ with random Ω. The prior of Ω is given in Section 2.3. The correlations among the $\gamma_{i,j}$s induce dependence among the outcomes within a patient, and the joint distribution of $(\tilde{\boldsymbol{Y}}_i, \boldsymbol{Z}_i)$ is obtained by integrating over $\boldsymbol{\gamma}_i$, as

$$p(\tilde{\boldsymbol{y}}_i, \boldsymbol{z}_i|d_{[i]}, \boldsymbol{\theta}, \tilde{\boldsymbol{\theta}}) = \int_{\mathbb{R}^4} p(\boldsymbol{y}_i, \boldsymbol{z}_i|d_{[i]}, \boldsymbol{\gamma}_i, \boldsymbol{\theta}, \tilde{\boldsymbol{\theta}}) \times p(\boldsymbol{\gamma}_i|\Omega)d\boldsymbol{\gamma}_i.$$

2.3 | Prior distributions and posterior computation

We specify priors for the model parameters $h_{0j}(t)$, $\boldsymbol{\beta} = (\beta_{\mathrm{PD}}, \beta_{\mathrm{T1}}, \beta_{\mathrm{T2}}, \beta_{\mathrm{T3}}, \beta_{\mathrm{D1}}, \beta_{\mathrm{D2}}, \beta_{\mathrm{D3}})$, ϕ, $\{\mu_\ell, \ell = 1, 2\}$, $\{\alpha_k, k = 2, 3\}$ and Ω as follows. We assume that h_{0j} is piecewise constant, which is a flexible function that can capture complex features of the hazard. To construct this, we fix the number of subintervals Q_j and cutoff points $s_{j,q}$, $q = 0, \ldots, Q_j$ placed evenly over $(0, C]$, that is, $s_{j,0} < s_{j,1} < s_{j,2} < \ldots < s_{j,Q_j}$ with $s_{j,0} = 0$, $s_{j,Q_j} = C$, and $s_{j,q+1} - s_{j,q} = C/Q_j$. For time t in subinterval $I_{j,q} = (s_{j,q-1}, s_{j,q}]$, we assume $h_{0j}(t) \equiv \lambda_{j,q}$. Denoting $\tilde{\lambda}_{j,q} = \log(\lambda_{j,q})$, we assume $\tilde{\lambda}_{j,1} \overset{indep}{\sim} \mathrm{N}(\tilde{\lambda}_{j,0}, \sigma_{j0}^2)$ and $\tilde{\lambda}_{j,q}|\tilde{\lambda}_{j,q-1} \overset{indep}{\sim} \mathrm{N}(\tilde{\lambda}_{j,q-1}, \sigma_j^2)$, $q = 2, \ldots, Q_j$ with fixed $\tilde{\lambda}_{j,0}$, σ_{j0}^2 and σ_j^2.[27] The resulting survival functions under this assumed piecewise constant hazard model given $\lambda_{j,q}$ are given in Supplementary Equations (2) and (3). Due to the discrete components of h_{0j}, the survival functions are discontinuous at the times $s_{j,q}$. Recall that we assume the relationships between dose and the outcomes, PD, and death can be either increasing or decreasing, while assuming the hazard of toxicity increases monotonically with dose. To ensure this, we assume either normal or truncated normal distributions for β accordingly. We assume normal distributions $\mathrm{N}(\overline{\beta}, \tau^2)$ for β_{PD}, β_{T2}, β_{D1}, and β_{D2}, and let β_{T3} and β_{D3} have normal distributions truncated above at 0, $p_j(\beta|\overline{\beta}, \tau^2) \propto \exp\{-(\beta - \overline{\beta})^2/(2\tau^2)\}$ for $\beta < 0$, $j = T3$, and $D3$. We assume β_{T1} follows a normal distribution truncated below at 0 so that $p_{\mathrm{T1}}(\beta|\overline{\beta}, \tau^2) \propto \exp\{-(\beta - \overline{\beta})^2/(2\tau^2)\}$ for $\beta > 0$ to impose a monotonic increasing relationship of toxicity with dose. For the parameters in the model for Z_ℓ, let $\xi_\ell|\overline{\xi}_\ell, \tau_{\xi\ell}^2 \overset{indep}{\sim} \mathrm{N}(\overline{\xi}_\ell, \tau_{\xi\ell}^2)$ for $\ell = 1, 2$ and $\phi|\overline{\phi}, \tau_\phi^2 \overset{indep}{\sim} \mathrm{N}\left(\overline{\phi}, \tau_\phi^2\right)$, and normal distributions with some restricted parameter space for α_k,

$$p(\alpha_2, \alpha_3|\overline{\boldsymbol{\alpha}}, \boldsymbol{\tau}_\alpha^2) \propto \prod_{k=2}^{3} \exp\{-(\alpha_k - \overline{\alpha}_k)^2/(2\tau_{\alpha k}^2)\}1(\alpha_k > \alpha_{k-1}),$$

with $\overline{\boldsymbol{\alpha}} = (\overline{\alpha}_2, \overline{\alpha}_3)$ and $\boldsymbol{\tau}_\alpha^2 = (\tau_{\alpha,2}^2, \tau_{\alpha,3}^2)$. The vector of all model parameters is $\boldsymbol{\theta} = (\tilde{\lambda}, \boldsymbol{\beta}, \boldsymbol{\xi}, \phi, \boldsymbol{\alpha})$, where $\tilde{\lambda} = \{\tilde{\lambda}_{j,q}, j = D, T, PD,$ and $q = 1, \ldots, Q_j\}$, $\boldsymbol{\xi} = (\xi_1, \xi_2)$, and $\boldsymbol{\alpha} = (\alpha_2, \alpha_3)$. Lastly, we define the prior of the covariance matrix for the

frailty vector $\Omega|\nu, \Omega^0 \sim$ inv-Wishart(ν, Ω^0) for fixed $\nu > 3$ and 4×4 positive definite hyperparameter matrix Ω^0. Collecting terms, the hyperparameter vector is $\tilde{\boldsymbol{\theta}} = (\tilde{\lambda}_0, \boldsymbol{\sigma}^2, \overline{\boldsymbol{\beta}}, \overline{\boldsymbol{\xi}}, \overline{\boldsymbol{\phi}}, \overline{\boldsymbol{\alpha}}, \boldsymbol{\tau}^2, \nu, \Omega^0)$, where $\tilde{\lambda}_0 = \{\tilde{\lambda}_{0j}, j = D, T, PD\}$, $\overline{\boldsymbol{\beta}} = \{\overline{\beta}_{\text{PD}}, \dots, \overline{\beta}_{\text{D3}}\}$, $\boldsymbol{\sigma}^2 = \{\sigma^2_{j0}, \sigma_j, j = D, T, PD\}$, and $\boldsymbol{\tau}^2 = \{\tau^2_{\text{D1}}, \dots, \tau^2_{\alpha 3}\}$.

To establish $\tilde{\boldsymbol{\theta}}$, we elicited probabilities of TTE outcomes within follow-up periods of 84 days for each of the nonfatal events PD and T and 365 days for D, and of the disease status outcomes evaluated by imaging at 42 and 84 days of follow-up. We then solved sets of equations under the assumed model to obtain prior means and calibrated dispersion parameters to reflect uncertainty in prior knowledge. Details of this process are given in Supplement Section 2.

Given $\tilde{\boldsymbol{\theta}}$ and interim data $\mathcal{D}_{n(t)}$ at trial time t, including all observed outcomes and dose assignments from previously enrolled patients, the joint posterior of the parameters $\boldsymbol{\theta}$ and patient-specific random effects $\boldsymbol{\gamma} = (\boldsymbol{\gamma}_1, \dots, \boldsymbol{\gamma}_{n(t)})$ is

$$p(\boldsymbol{\theta}, \boldsymbol{\gamma}|\mathcal{D}_{n(t)}, \tilde{\boldsymbol{\theta}}) \propto \prod_{i=1}^{n(t)} p(\tilde{\boldsymbol{y}}_i^o, \boldsymbol{z}_i, \boldsymbol{\delta}_i|d_{[i]}, \boldsymbol{\gamma}_i, \boldsymbol{\theta}, \tilde{\boldsymbol{\theta}})\ p(\boldsymbol{\theta}, \boldsymbol{\gamma}|\tilde{\boldsymbol{\theta}}), \tag{10}$$

where $p(\tilde{\boldsymbol{y}}_i^o, \boldsymbol{z}_i, \boldsymbol{\delta}_i|d_{[i]}, \boldsymbol{\gamma}_i, \boldsymbol{\theta}, \tilde{\boldsymbol{\theta}})$ is specified in Equation (9). We use Markov chain Monte Carlo (MCMC) simulation to generate posterior samples of $\boldsymbol{\theta}$ and $\boldsymbol{\gamma}$. Computational details are given in Supplement Section 1. Data sharing is not applicable to this paper as all data in Section 4 is computer simulated. An R package "DosefindingPeriodicEff" for implementing this methodology for simulated data is available from https://github.com/juheelee2/DosefindingPeriodicEff.

3 | TRIAL DESIGN

3.1 | Utility function

Our proposed design uses an elicited utility function of $(\boldsymbol{Y}, \boldsymbol{Z})$ on a finite number of sets defined in terms of subintervals that partition the follow-up period $(0, C]$. In the application, the subintervals are (0, 42] and (42, 84]. Denote $a_D = 1$ if $Y_{\text{D}} \leq 84$ and $a_D = 2$ if $Y_{\text{D}} > 84$. We first assign utility 0 to any outcome $(\boldsymbol{Y}, \boldsymbol{Z})$ where the patient dies during follow-up, $(Y_D \leq 84) = (a_D = 1)$. Given this, we define 11 events for efficacy, identified by $a_{\text{PD}} = 1, \dots, 11$, as combinations of Y_{PD} and (Z_1, Z_2), and three events for toxicity, identified by $a_{\text{T}} = 1, 2, 3$. For patients who survive the 84 day follow-up period, the 33 elementary events $\boldsymbol{a} = (a_{\text{PD}}, a_{\text{T}}, a_{\text{D}})$ with $a_{\text{D}} = 2$ determined by combining these variables are given in Table 1, along with the elicited utility $U(\boldsymbol{a})$ of each $\boldsymbol{a}$. The numerical values reflect the fact that, given $U(\boldsymbol{a}) = 0$ if $Y_{\text{D}} \leq C$, having neither toxicity nor PD during the follow-up and CR for at both 42 and 84 days is the best outcome ($U = 100$). Having severe toxicity or PD earlier during the follow-up is worse, and better response evaluation scores from imaging have larger utilities.

Given $\boldsymbol{\theta}$, we evaluate probabilities of each $\boldsymbol{a}$ for each dose d_m in terms of $\Pr(\boldsymbol{Y}, \boldsymbol{Z}|d_m, \boldsymbol{\theta})$, and compute the mean utility. For example,

$$\begin{aligned}\Pr\{\boldsymbol{a} = (8, 2, 2)|d_m, \boldsymbol{\theta}\} &= \Pr\{Y_{\text{PD}} > 84, \boldsymbol{Z} = (2, 3), Y_{\text{T}} \in (42, 84], Y_{\text{D}} > 84|d_m, \boldsymbol{\theta}\} \\ &= \int_{84}^{\infty} \int_{42}^{84} \int_{84}^{\infty} \int_{\mathbb{R}^4} p(\boldsymbol{y}, \boldsymbol{Z} = (2, 3)|d_m, \boldsymbol{\gamma}, \boldsymbol{\theta}) p(\boldsymbol{\gamma}|\boldsymbol{\theta}) d\boldsymbol{\gamma}\ d\boldsymbol{y}.\end{aligned}$$

Given $\boldsymbol{\theta}$, the mean utility of assigning dose d_m to a future patient is

$$\bar{U}(d_m, \boldsymbol{\theta}) = \sum_{a_{\text{PD}}=1}^{11} \sum_{a_{\text{T}}=1}^{2} U(a, b, 2)\ \Pr(\boldsymbol{a} = (a_{\text{PD}}, a_{\text{T}}, 2)|d_m, \boldsymbol{\theta}). \tag{11}$$

A frequentist approach might compute a plug-in estimator, $\hat{\boldsymbol{\theta}}$ and use $\bar{U}(d_m, \hat{\boldsymbol{\theta}})$ as a dose selection criteria. Instead, we exploit the posterior predictive distribution, defined within the Bayesian structure. Given data $\mathcal{D}_{n(t)}$ at trial time t, the posterior predictive mean utility of giving dose d_m to a future patient is

$$u(d_m|\mathcal{D}_{n(t)}) = \int_{\boldsymbol{\theta}} \bar{U}(d_m, \boldsymbol{\theta}) p(\boldsymbol{\theta}|\mathcal{D}_{n(t)}) d\boldsymbol{\theta}. \tag{12}$$

This maps the elicited outcome utilities in Table 1 and the current data to a set of posterior mean utilities, one for each dose. We will use this as an optimality criterion for dose assignment during the trial, and for final dose selection at its completion. While utilities are elicited for events occurring or not during the follow-up interval, to improve reliability, all follow-up information on $(\tilde{\boldsymbol{Y}}_i, \boldsymbol{Z}_i, \boldsymbol{\delta}_i)$, for $i = 1, \ldots, n(t)$ is used to compute $u(d_m|\mathcal{D}_{n(t)})$, using the empirical mean of a posterior sample of $\boldsymbol{\theta}$ values simulated from $p(\boldsymbol{\theta}|\mathcal{D}_{n(t)}, \tilde{\boldsymbol{\theta}})$ using MCMC. Details are given in Supplementary Section 1.

3.2 | Dose acceptability and adaptive randomization

While the posterior predictive mean utility in Equation (12) is used as an optimality criterion, we do not fully trust the utility function to protect patient safety. The aim of the metastatic renal cancer trial is to find the optimal dose of sitravatinib from the four levels 60, 80, 120, and 150 mg given orally each day until PD, when combined with nivolumab given at a fixed dose of 240 mg intravenously every two weeks until PD. Since lower doses may carry a higher risk of death or PD, and higher doses carry a higher risk of toxicity, we will restrict the set of acceptable doses by imposing the following safety conditions.

The first safety criterion is the commonly used constraint that an untried dose may not be skipped when escalating. Formally, if $d_{m^{\max}(t)}$ is the highest dose level that has been administered by trial time t, then the search for the optimal dose is constrained so that $d_m \in \mathcal{A}^{\text{Tried}}(t) = \{d_1, \ldots, d_{\min\{(m^{\max}(t)+1),\ M\}}\}$. In addition, we monitor safety and efficacy to avoid giving patients undesirable doses, as follows. For each d_m, we denote the probabilities of observing PD, T, or D during the full 12-week (84-day) follow-up period by

$$\begin{aligned}
\zeta_{\text{PD}}(d_m, \boldsymbol{\theta}) &= \Pr\{Y_{\text{PD}} \le \min(C, Y_{\text{D}}),\ \text{ or } Z_\ell = 0 \text{ for any } \ell | d_m, \boldsymbol{\theta}\},\\
\zeta_{\text{T}}(d_m, \boldsymbol{\theta}) &= \Pr\{Y_{\text{T}} \le \min(C, Y_{\text{D}}) | d_m, \boldsymbol{\theta}\},\\
\zeta_{\text{D}}(d_m, \boldsymbol{\theta}) &= \Pr(Y_{\text{D}} \le C | d_m, \boldsymbol{\theta}).
\end{aligned}$$

For each outcome $j = PD, T, D$, let $\overline{\zeta}_j$, be an elicited fixed upper limit on $\zeta_j(d_m, \boldsymbol{\theta})$, and let $p^\star$ be a fixed cut-off probability. During the trial, if

$$\text{P}\{\zeta_j(d_m, \boldsymbol{\theta}) > \overline{\zeta}_j \text{ for } j = PD,\ T, \quad \text{or } D | \mathcal{D}_{n(t)}\} > p^\star, \tag{13}$$

then d_m is considered unacceptable and is not administered. We let $\mathcal{A}^{\text{Accp}}(t)$ denote the set of acceptable doses at time t, which do not satisfy the criterion in Equation (13). The elicited values $\overline{\zeta}_{\text{D}} = 0.30$, $\overline{\zeta}_{\text{T}} = 0.40$ and $\overline{\zeta}_{\text{PD}} = 0.70$ for the renal cancer trial were provided by the clinical investigators. The limit $\overline{\zeta}_{\text{D}} = 0.30$ was motivated by the fact that less than 30% of metastatic renal cancer patients treated with single-agent nivolumab, the immunotherapy serving as the backbone for the targeted agent sitravatinib added to the regimen, will die within 12 weeks of enrollment. If a combination dose is associated with ≥30% of patients dying within 12 weeks, then that dose is unacceptable. The limit $\overline{\zeta}_{\text{T}} = 0.40$ was determined from the consideration that, regardless of what the efficacy outcome may be, it is unacceptable for ≥ 40% of patients to develop dose-limiting toxicity within 12 weeks. The apparently very high limit $\overline{\zeta}_{\text{PD}} = 0.70$ was set because it is expected that the single-agent nivolumab should produce SD, PR, or CR in at least 20-30% of patients within 12 weeks, so adding sitravatinib should not be permitted to do worse. To obtain a design with high probabilities of stopping a truly unsafe or inefficacious dose, and of selecting the best safe and efficacious dose, we investigated cut-offs 0.75, 0.80, and 0.85 by simulation, and chose $p^\star = 0.80$.

At trial time t, the safety and efficacy constraints together define a set of acceptable doses $\mathcal{A}(t) = \mathcal{A}^{\text{Tried}}(t) \cap \mathcal{A}^{\text{Accp}}(t) \subseteq \{d_1, \ldots, d_M\}$ based on interim data $\mathcal{D}_{n(t)}$. To produce reliable decisions, we let $\mathcal{A}(t) = \mathcal{A}^{\text{Tried}}(t)$ early in a trial due to insufficient data. The dose acceptability monitoring is begun when at least 20 patients have died or been fully followed for 84 days. We chose the value 20 based on preliminary trial simulations, in which the designs with the values 15, 20, and 25 were evaluated. In terms of the utility-based objective function, the dose that maximizes $u(d_m|\mathcal{D}_{n(t)})$ yields the best clinical outcomes. However, the reliability of the process over the entire trial can be improved by including adaptive randomization (AR). Thus, during trial conduct, patients are adaptively randomized among $d_m \in \mathcal{A}(t)$. Using AR decreases the probability of the sequential algorithm getting stuck at a suboptimal dose, and also has the effect of treating more patients at doses having larger utilities, on average. See, for example, Thall and Nguyen,[28] Yan et al,[29] or Chapple and Thall.[30] Specifically, we assign a patient dose $d_m \in \mathcal{A}(t)$ with probability proportional to $u(d_m|\mathcal{D}_{n(t)})$. If $\mathcal{A}(t) = \emptyset$,

then we terminate the trial and no dose is selected, $d_{\text{sel}} = None$. To determine a final optimal action when $N_{\max} = 60$ at $T_{\max} = e_{N_{\max}} + C$, we identify $\mathcal{A}(T_{\max})$. If $\mathcal{A}(T_{\max}) = \emptyset$, then $d_{\text{sel}} = None$, while if $\mathcal{A}(T_{\max}) \neq \emptyset$, then the selected optimal dose is $d_{\text{sel}} = \arg\max_{d_m \in \mathcal{A}(T_{\max})} u(d_m | \mathcal{D}_{N_{\max}})$.

4 | SIMULATION STUDY

4.1 | Simulation design

To evaluate the design's performance, we simulated the renal cancer trial under 10 dose-outcome scenarios. Due to the complexity of the outcome structure, constructing simulation scenarios is not entirely straightforward. For each scenario, we first specified marginal occurrence probabilities $\tilde{p}_{j,d_m} = \text{P}(Y_j < C | d_m)$, $j = PD, T, D$ and $d_m \in \{d_1, \ldots, d_4\}$ for $M = 4$ doses that ignore both dependent censoring by death and the two separate PD observation processes. We also specified the covariance matrix Ω^{true} for the frailty vectors and simulated frailties $\boldsymbol{\gamma}_i^{\text{true}} \overset{iid}{\sim} \text{N}_4(\mathbf{0}, \Omega^{\text{true}})$.

Given $d_{[i]}$, $\boldsymbol{\gamma}_i^{\text{true}}$ and $\tilde{p}_{j,d_{[i]}}$, we generated event times $Y_{i,j}, j = T$ and D, from the Weibull distribution with shape parameter $\chi_{i,j}^{\text{true}}$ and scale parameter $g_{i,j} \exp(\gamma_{i,j}^{\text{true}})$, where $g_{i,j}$ is the solution of the equation, $\tilde{p}_{j,d_{[i]}} = 1 - \exp(g_{i,j} \times C_j^{\chi_{i,j}^{\text{true}}})$. That is, in the simulation truth, the dose-outcome relationship was specified arbitrarily through $\tilde{p}_{j,d_m}$ and the hazards are continuous in time. In contrast, for the design, the dose-response relationship is modeled through assumed parametric function η_j and discontinuous hazards. Thus, our modeling assumptions are very different from the simulation truth, so the simulation examines robustness of our design. To simulate $Y_{i,\text{PD}}$ and $\boldsymbol{Z}_i$, we utilized a probit model that allows an arbitrary relationship between d and Z. We specified ϕ^{true} and $\tilde{\pi}_{1,k}(d_1)$, $k = 0, \ldots, 3$ and $\sigma_\pi^{2,\text{true}}$ and found the quantiles to fix the true cutoff values $u_k^{\text{true}} = \Phi^{-1}\left(\sum_{k'=0}^{k-1} \tilde{\pi}_{1,k'}(d_1) | 0, \sigma_\pi^{2,\text{true}} \right)$, $k = 1, 2, 3$, with $u_0^{\text{true}} = -\infty$ and $u_4^{\text{true}} = \infty$, where $\Phi^{-1}(\cdot | a, b^2)$ is the quantile function of $\text{N}(a, b^2)$. We set $\xi_1^{\text{true}} = -d_1 \times \phi^{\text{true}}$ and specified ξ_2^{true}. We then computed

$$\begin{aligned}
\pi_{1,k}^{\text{true}}(d_{[i]}, \boldsymbol{\gamma}_i^{\text{true}}) &= \Phi\left(u_{k+1}^{\text{true}} | \xi_1^{\text{true}} + \phi^{\text{true}} d_{[i]} + \gamma_{i,\text{Z}}^{\text{true}}, \sigma_\pi^{2,\text{true}} \right) \\
&\quad - \Phi\left(u_k^{\text{true}} | \xi_1^{\text{true}} + \phi^{\text{true}} d_{[i]} + \gamma_{i,\text{Z}}^{\text{true}}, \sigma_\pi^{2,\text{true}} \right), \quad \text{and} \\
\pi_{2,k}^{\text{true}}(d_{[i]}, Z_{i,1}, \boldsymbol{\gamma}_i^{\text{true}}) &= \Phi\left(u_{k+1}^{\text{true}} | \xi_2^{\text{true}} + \phi^{\text{true}} d_{[i]} + \alpha_{Z_{i,1}}^{\text{true}} + \gamma_{i,\text{Z}}^{\text{true}}, \sigma_\pi^{2,\text{true}} \right) \\
&\quad - \Phi\left(u_k^{\text{true}} | \xi_2^{\text{true}} + \phi^{\text{true}} d_{[i]} + \alpha_{Z_{i,1}}^{\text{true}} + \gamma_{i,\text{Z}}^{\text{true}}, \sigma_\pi^{2,\text{true}} \right).
\end{aligned}$$

We let $S_{\text{PD},i}^{\prime,\text{true}}(t) = \exp\{-g_{i,\text{PD}} \exp(\gamma_{i,\text{PD}})\} t^{\chi_{i,\text{PD}}^{\text{true}}}$, where $\chi_{i,\text{PD}}^{\text{true}}$ is specified and $g_{i,\text{PD}}$ is the solution of the equation $\tilde{p}_{\text{PD},d_{[i]}} = 1 - \exp(g_{i,\text{PD}} \times C_{\text{PD}}^{\chi_{i,\text{PD}}^{\text{true}}})$. Finally, we simulated $Y_{i,\text{PD}}$ and $\boldsymbol{Z}_i$ using the mixed hazard in Equation (6) with $S_{\text{PD},i}^{\prime,\text{true}}(t)$, $\pi_{1,k}^{\text{true}}(d_{[i]}, \boldsymbol{\gamma}_i^{\text{true}})$ and $\pi_{2,k}^{\text{true}}\left(d_{[i]}, Z_1, \boldsymbol{\gamma}_i^{\text{true}}\right)$. Similar to the true model for Y_{D} and Y_{T}, the true model of Y_{PD} and Z_ℓ is more complex than the assumed regression model for the design. In particular, the true cutoff points can be very different from the assumed cutoff points. We assumed $e_i - e_{i-1} | e_{i-1} \overset{iid}{\sim} \text{Exp}(1/30)$ with $e_0 = 0$ and simulated random imaging times $t_{i,1}^\star = 38 + 9 \times v_{i,1}$ and $t_{i,2}^\star = 80 + 9 \times v_{i,2}$ with $v_{i,\ell} \overset{iid}{\sim} \text{Be}(2.4, 2.4)$. This lets a new patient to be treated every 30 days, on average, and $t_{i,1}^\star = 42.5 \pm 3.5$ days and $t_{i,2}^\star = 84.5 \pm 3.5$ days. For Scenarios 1-9, we assumed $\chi_{i,j}^{\text{true}} = 1.0$, 0.7 and 1.3 for $j = PD, T, D$, corresponding to hazard functions constant, decreasing and increasing in time, respectively, for all i. For Scenario 10, we assumed nonmonotone baseline hazard functions in the truth by using a mixture of two Weibull distributions; we let $\chi_{i,j}^{\text{true}} = 0.7$ or 1.3 with equal probability for all (i, j). We also let $\sigma_\pi^{2,\text{true}} = 1.5$ and $\Omega_{j,j}^{\text{true}} = 0.1, j = 1, \ldots, 4, \Omega_{j,4}^{\text{true}} = -0.05$ and $\Omega_{j,j'}^{\text{true}} = 0.05, j \neq j', j' \neq 4$ for Ω^{true} for all scenarios. Supplementary Tables 3 and 4 show the assumed values of $\tilde{p}_{j,d}$, $\tilde{\pi}_{1,0}(d_m)$, ϕ^{true}, ξ_ℓ^{true}, and α_z^{true} for each of the scenarios. Supplementary Table 3 also illustrates the expected numbers of observing any $Z_\ell = z$, $\overline{\pi}_{\bullet 0}(d_m) = \pi_{1,z}^{\text{true}}(d_m, \boldsymbol{\gamma})$ and $\overline{\pi}_{\bullet z}(d_m) = \pi_{1,z}^{\text{true}}(d_m, \boldsymbol{\gamma}) + \sum_{z_1=1}^{3} \pi_{1,z_1}^{\text{true}}(d_m, \boldsymbol{\gamma}) \pi_{2,z}^{\text{true}}(d_m, z_1, \boldsymbol{\gamma})$, $z \neq 0$, with $\gamma_Z = 0$. The scenarios assume various dose effect patterns. For example, some scenarios have patterns that increase and then plateau, for example, $\tilde{p}_{\text{T}}$ in Scenario 1 and $\tilde{p}_j$ for all outcomes in Scenario 10. Also, $\tilde{p}_{\text{D}}$ in Scenario 9 decreases and then increases in dose, which violates the model assumption in Equation (8). Details of the simulation design are given in Supplementary Section 3.

The specified marginal probabilities $\tilde{p}_{j,d_m}$ are not the same as $p_{j,d_m}^{\text{true}} = \text{P}^{\text{true}}(\delta_j = 1 | d_m)$ due to marginalization over random frailties and the semicompeting structure. We numerically evaluate the true probabilities of observing events

$p^{\text{true}}_{j,d_m} = \text{P}^{\text{true}}(\delta_j = 1|d_m)$ and true expected utilities $U^{\text{true}}(d_m)$ using a Monte Carlo method. Table 3 gives p^{true}_{j,d_m} and $U^{\text{true}}(d_m)$ for each scenario, with truly unacceptable doses and optimal doses given in red and blue, respectively. Recall the elicited thresholds $\overline{\zeta}_{\text{PD}} = 0.70$, $\overline{\zeta}_{\text{T}} = 0.40$, and $\overline{\zeta}_{\text{D}} = 0.30$. In Scenarios 1-4, while the probability of toxicity is kept stable in doses, the probabilities of PD and death vary and modeling death and PD accurately is critical in making correct decisions. In Scenarios 1 and 2, all doses are safe, and the true optimal doses are doses 1 and 4 due to the changing patterns in the probabilities of PD and death over doses, respectively. In Scenarios 3 and 4, all doses are unacceptable due to excessive probabilities of death and PD, respectively. Scenarios 5-8 have respective truly optimal doses, 1, 2, 3, 4, with some of the other doses unacceptable. For those scenarios, it is important to fully use ordinal response outcomes to select true optimal doses with high accuracy. For example, in Scenario 8, $\overline{\pi}_{\bullet 3}$ increases a lot for dose 4 (0.05, 0.19, 0.38, and 0.80 for doses 1-4, respectively), resulting in dose 4 being the optimal, despite of increasing toxicity probabilities. A total of $R = 500$ trials were simulated under each scenario.

As a comparator, described briefly in Section 1, we used a design with two time to event outcomes. We defined the time to severe toxicity in the same way, so $Y'_{\text{T}} = Y_{\text{T}}$, but defined Y'_{PD} to be the time to PD or death, ignoring whether PD is observed from Y_{PD} or $\boldsymbol{Z}$. Under the comparator, efficacy represents the event that the patient is alive without PD at day 84, $[Y'_{\text{PD}} > 84]$. Thus, nonefficacy can be observed at any time up to day 84, but efficacy cannot be known to have occurred before day 84. This sort of combination of two or more actual outcomes to define a single efficacy or toxicity variable is very common in phase I-II designs. Based on $(Y'_{\text{PD}}, Y'_{\text{T}})$, the reduced outcome design assumes PH models with piecewise constant baseline hazards h'_{0j} and logistic functions for the dose-outcome relationship $\eta'_j(d, \boldsymbol{\gamma}') = \frac{\beta'_{j3}}{1+\exp(\beta'_{j1}\times(10\times d-\beta'_{j2}))} + \gamma'_j$ for $j = PD, T$, where $\boldsymbol{\gamma}' = (\gamma'_{\text{PD}}, \gamma'_{\text{T}})$, similar to Equation (1). As in the full outcome model, we let $\beta'_{j2} \in \mathbb{R}$ and $\beta'_{j3} < 0$ for $j = PD$ and T and assume dose coefficients $\beta'_{\text{PD1}} \in \mathbb{R}$ and $\beta'_{\text{T1}} > 0$. We also assume normal priors for $\boldsymbol{\beta}'_j$, and an inverse Wishart prior for Ω'. Fixed prior hyperparameters under the reduced outcome model were specified by using the same elicited prior probabilities. Under the reduced outcome design, we defined $\mathcal{A}^{\text{Accp}}(t)$ as the set of doses that do not satisfy

$$\text{P}\{\zeta'_j(d, \boldsymbol{\theta}') > \overline{\zeta}'_j, \quad \text{for } j = PD \text{ or } T|\mathcal{D}_{n(t)}\} > p^\star, \quad j = PD \quad \text{or} \quad T,$$

where $\zeta'_j(d, \boldsymbol{\theta}') = \text{P}(\delta_j = 1|d, \boldsymbol{\theta}')$. We used $\overline{\zeta}'_{\text{PD}} = 0.79$ and $\overline{\zeta}'_{\text{T}} = 0.4$, which provides a comparable threshold for Y'_{PD}. Utilities were elicited for reduced outcomes $(Y'_{\text{PD}}, Y_{\text{T}})$, and shown in Table 2. A key difference between the full and reduced outcome utilities is that there are 33 elementary events of $\boldsymbol{a}$ with $a_{\text{D}} = 2$ in the partition based on $(\boldsymbol{Y}, \boldsymbol{Z})$, but only nine elementary events $(a'_{\text{PD}}, a_{\text{T}})$ in the partition based on $(Y'_{\text{PD}}, Y_{\text{T}})$. As in the full outcome design, posterior mean utility was used to perform AR during the trial and to choose an optimal dose at the end. The reduced outcome design is more sophisticated than most phase I-II designs, but it still does not fully utilize all observables available during the trial. Under the reduced outcome model, patterns of the expected utilities over doses or optimal doses may be different from those in the truth because it is poorly informed by the simplified outcomes $(Y'_{\text{PD}}, Y_{\text{T}})$. As the examples given in Section 1 illustrate and our simulations will show, the reduced outcome design often makes bad decisions.

In the simulations, we evaluated the full and reduced outcome designs using three criteria, $p^{\text{unacc}} = \Pr$(declaring a dose unacceptable), in terms of having an excessive probability of PD, severe toxicity, or death, $p^{\text{sel}} = \Pr$(selecting a dose as optimal) and $p^{\text{ptrt}} = \Pr$(treating a patient in trial at a given dose). For each simulated trial $r = 1, \ldots, R$ under each design and dose-outcome scenario, we denote by $d_{\text{sel},r}$ the dose selected by each design. We let $\kappa_{r,m} = 1$ if dose d_m is identified as unacceptable in simulated trial r, or 0 if not, and the number of patients treated in trial r denoted by N_r. Denoting the indicator function of event A by $\text{I}(A)$, for each dose d_m, $m = 1, 2, 3, 4$, we summarized simulation results by computing the empirical proportions across the R simulated trials,

$$p^{\text{unacc}} = \frac{\sum_{r=1}^{R} \kappa_{r,m}}{R}, \quad p^{\text{sel}} = \frac{\sum_{r=1}^{R} \text{I}(d_{\text{sel},r} = d_m)}{R}, \quad p^{\text{ptrt}} = \frac{\sum_{r=1}^{R} \sum_{i=1}^{N_r} \text{I}(d_{r,[i]} = d_m)}{\sum_{r=1}^{R} N_r}.$$

4.2 | Simulation results

The simulation results are summarized in Table 3, including the true values $p^{\text{true}}_{\text{PD}}$, $p^{\text{true}}_{\text{T}}$, and $p^{\text{true}}_{\text{D}}$ for each dose to facilitate evaluation. Overall, the full outcome design reliably identifies doses that are unsafe or have very low efficacy and selects optimal acceptable doses, based on $N_{\max} = 60$. Large p^{unacc}_m is achieved for doses having large $p^{\text{true}}_{\text{PD}}$, $p^{\text{true}}_{\text{T}}$ or $p^{\text{true}}_{\text{D}}$. When

TABLE 3 Simulation results for the full outcome and reduced outcome designs

		d_1	d_2	d_3	d_4	*None*	d_1	d_2	d_3	d_4	None
		Scenario 1					Scenario 2				
p_{PD}^{true}		0.58	0.50	0.41	0.36		0.65	0.35	0.08	0.05	
p_{T}^{true}		0.05	0.05	0.10	0.09		0.01	0.03	0.08	0.10	
p_{D}^{true}		0.01	0.15	0.20	0.25		0.01	0.05	0.10	0.15	
U^{true}		**52.39**	44.85	42.97	40.87		51.78	54.64	65.40	**73.00**	
Full	p^{unacc}	0.04	0.02	0.09	0.14		0.08	0.00	0.00	0.01	
Outcome	p^{sel}	**0.77**	0.16	0.01	0.05	0.02	0.00	0.02	0.05	**0.93**	0.00
	p^{ptrt}	**0.30**	0.28	0.22	0.18	0.01	0.23	0.25	0.26	**0.26**	0.00
Reduced	p^{unacc}	0.00	0.00	0.01	0.02		0.00	0.00	0.00	0.00	
Outcome	p^{sel}	**0.52**	0.07	0.10	0.31	0.00	0.00	0.04	0.32	**0.64**	0.00
	p^{ptrt}	**0.28**	0.26	0.24	0.22	0.00	0.25	0.25	0.26	**0.24**	0.00
		Scenario 3					Scenario 4				
p_{PD}^{true}		0.47	0.49	0.50	0.55		*0.91*	*0.91*	*0.88*	*0.83*	
p_{T}^{true}		0.19	0.20	0.29	0.31		0.05	0.10	0.16	0.21	
p_{D}^{true}		*0.65*	*0.55*	*0.50*	*0.40*		0.15	0.10	0.05	0.01	
U^{true}		15.81	20.37	21.67	26.39		38.31	40.24	43.25	46.17	
Full	p^{unacc}	*1.00*	*1.00*	*1.00*	*1.00*		*1.00*	*1.00*	*0.92*	*0.81*	
Outcome	p^{sel}	0.00	0.00	0.00	0.00	**1.00**	0.00	0.00	0.00	0.18	**0.81**
	p^{ptrt}	0.11	0.10	0.10	0.10	**0.60**	0.12	0.10	0.12	0.19	**0.46**
Reduced	p^{unacc}	*0.88*	*0.84*	*0.78*	*0.77*	*0.97*	*0.91*	*0.27*	*0.22*		
Outcome	p^{sel}	0.06	0.05	0.03	0.17	**0.68**	0.00	0.01	0.11	0.66	**0.21**
	p^{ptrt}	0.17	0.16	0.16	0.16	**0.34**	0.13	0.14	0.30	0.32	**0.11**
		Scenario 5					Scenario 6				
p_{PD}^{true}		0.55	0.44	0.36	0.26		0.63	0.44	0.24	0.14	
p_{T}^{true}		0.01	0.10	0.24	0.27		0.05	0.05	0.33	*0.57*	
p_{D}^{true}		0.03	0.15	0.20	*0.30*		0.05	0.05	0.25	*0.40*	
U^{true}		**52.54**	45.48	42.23	37.94		54.20	**62.12**	54.22	45.35	
Full	p^{unacc}	0.01	0.01	0.15	*0.26*		0.01	0.00	0.52	*0.87*	
Outcome	p^{sel}	**0.81**	0.17	0.01	0.01	0.00	0.02	**0.80**	0.13	0.05	0.00
	p^{ptrt}	**0.32**	0.30	0.22	0.16	0.00	0.35	**0.37**	0.19	0.09	0.00
Reduced	p^{unacc}	0.00	0.00	0.04	*0.07*		0.01	0.00	0.34	*0.69*	
Outcome	p^{sel}	**0.71**	0.13	0.04	0.12	0.00	0.18	**0.68**	0.11	0.03	0.00
	p^{ptrt}	**0.3**	0.27	0.23	0.21	0.00	0.33	**0.33**	0.21	0.13	0.00

(Continues)

TABLE 3 (Continued)

		d_1	d_2	d_3	d_4	*None*	d_1	d_2	d_3	d_4	None
		Scenario 7					Scenario 8				
$p_{\text{PD}}^{\text{true}}$		0.45	0.24	0.13	0.08		*0.88*	*0.81*	0.60	0.39	
$p_{\text{T}}^{\text{true}}$		0.10	0.15	0.20	0.31		0.01	0.05	0.20	0.30	
$p_{\text{D}}^{\text{true}}$		0.05	0.10	0.15	*0.35*		0.10	0.10	0.05	0.05	
U^{true}		57.40	64.33	**73.46**	57.34		42.43	43.93	52.76	**61.26**	
Full	p^{unacc}	0.00	0.00	0.08	*0.35*		*0.83*	*0.38*	0.07	0.08	
	p^{sel}	0.01	0.23	**0.60**	0.16	0.00	0.00	0.01	0.03	**0.91**	0.06
	p^{ptrt}	0.28	0.29	**0.25**	0.18	0.00	0.14	0.20	0.31	**0.32**	0.03
Reduced	p^{unacc}	0.00	0.00	0.02	*0.09*		*0.50*	*0.33*	0.04	0.05	
	p^{sel}	0.35	0.29	**0.25**	0.11	0.00	0.00	0.02	0.12	**0.83**	0.03
	p^{ptrt}	0.29	0.27	**0.24**	0.20	0.00	0.19	0.20	0.30	**0.29**	0.02
		Scenario 9					Scenario 10				
$p_{\text{PD}}^{\text{true}}$		0.68	0.62	0.46	0.41		0.57	0.50	0.39	0.35	
$p_{\text{T}}^{\text{true}}$		0.05	0.05	0.28	0.28		0.01	0.10	0.27	0.27	
$p_{\text{D}}^{\text{true}}$		0.10	0.05	0.25	0.25		0.03	0.15	0.25	0.25	
U^{true}		48.37	**53.78**	42.76	46.04		**51.90**	44.38	38.09	38.85	
Full	p^{unacc}	0.08	0.04	0.23	0.34		0.05	0.03	0.22	0.31	
	p^{sel}	0.13	**0.62**	0.02	0.20	0.03	**0.81**	0.12	0.00	0.04	0.03
	p^{ptrt}	0.30	**0.30**	0.21	0.17	0.02	**0.33**	0.30	0.20	0.16	0.02
Reduced	p^{unacc}	0.02	0.01	0.10	0.15		0.00	0.00	0.06	0.09	
	p^{sel}	0.34	**0.32**	0.05	0.29	0.00	**0.76**	0.08	0.03	0.13	0.00
	p^{ptrt}	0.29	**0.28**	0.23	0.20	0.00	**0.30**	0.28	0.23	0.19	0.00

Note: p_m^{unacc} = P(declare dose m unacceptable), p_m^{sel} = P(select dose m as optimal), and p_m^{ptrt} = P(treat a patient at dose m), are illustrated for Scenarios 1-6 under the proposed design (full Outcome) and the reduced outcome design (reduced Outcome). Values for *true unacceptable* and **true optimal** doses are given in *red italic* and **blue bold**, respectively. $\overline{\zeta}_{\text{PD}} = 0.70$, $\overline{\zeta}_{\text{T}} = 0.40$, and $\overline{\zeta}_{\text{D}} = 0.30$ are the fixed upper limits used to define acceptability.

either of $p_{\text{PD}}^{\text{true}}$ or $p_{\text{T}}^{\text{true}}$ is clearly greater than its fixed upper threshold $\overline{\zeta}_j$, p_m^{unacc} is particularly high. When all doses are unacceptable, as in Scenarios 3 and 4, p_m^{unacc} is especially high for all m, because the full outcome model borrows information across doses through η_j and thus improves reliability. The design is likely to identify unacceptable doses even in scenarios where only some doses are unacceptable, as in Scenarios 5-8. In some scenarios, acceptable doses whose true probabilities are close to the threshold $\overline{\zeta}_j$ do not have very large p^{unacc}, as in the case with d_4 in Scenario 7, due in part to the small sample size. When all doses are truly unacceptable, trials are stopped or conclude no optimal dose with high probability. In Scenarios 3 and 4, the design identifies the doses as unacceptable and terminates trials early or selects no dose 100% and 81% of the time, respectively. For the remaining scenarios, p_m^{sel} is larger at least as 60% for the true optimal doses. Scenarios 1, 2, 5-8, and 10 have $p_m^{\text{sel}} = 77\%$, 93%, 81%, 80%, 60%, 91%, and 81%, respectively, showing that the full outcome design performs very well in optimal dose selection. In addition, the proportions p_m^{ptrt} of patients treated at d_m in the trial show that the design reliably identifies unacceptable doses during a trial and assigns fewer patients to truly unacceptable doses. For example, 60% and 46% of patients were not treated in Scenarios 3 and 4. In Scenarios 5-8, fewer patients were treated at their unsafe doses, and more patients were treated at the truly optimal or truly safe doses. Recall that the true probabilities of observing events during the follow-up period, $p_{\text{PD},d_m}^{\text{true}}$, $p_{\text{T},d_m}^{\text{true}}$, and $p_{\text{D},d_m}^{\text{true}}$, are arbitrarily specified for doses, whereas the design assumes PH models with regression functions for dose-outcome relationship. Especially in Scenario 9, the pattern of $\tilde{p}_{\text{D}}$ over d_m is not monotone, which violates the model assumption. It thus is remarkable that, in terms of all criteria, the proposed design performs well in the various scenarios.

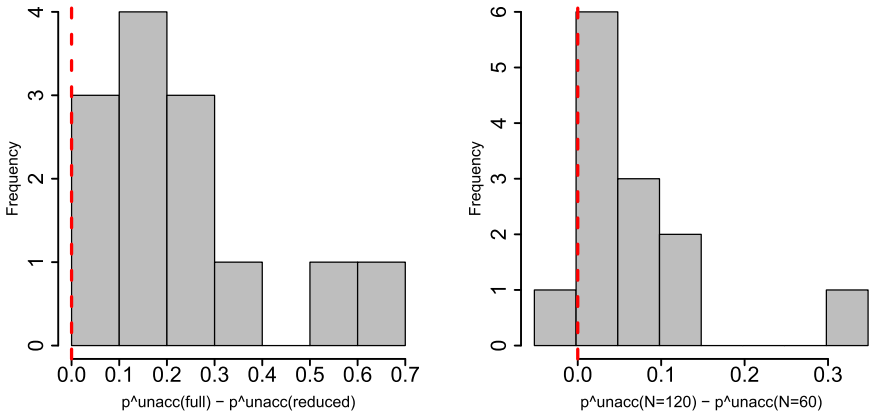

(A) Full vs Reduced Designs (B) $N_{\max} = 120$ vs 60

FIGURE 3 [Safety: Comparison of probabilities of identifying truly unacceptable doses] Histograms of differences in p_m^{unacc} for truly unacceptable doses for all scenarios combined. Histograms of, A, $p_m^{\text{unacc}}(\text{N} = 60, \text{Full}) - p_m^{\text{unacc}}(\text{N} = 60, \text{Reduced})$ and, B, $p_m^{\text{unacc}}(\text{N} = 120, \text{Full}) - p_m^{\text{unacc}}(\text{N} = 60, \text{Full})$. Larger positive values correspond to superior performance in identification of unacceptable doses by the Full versus Reduced outcome design with $N = 60$ patients in (A), and of maximum sample size 120 versus 60 for the Full outcome design in (B) [Colour figure can be viewed at wileyonlinelibrary.com]

The reduced outcome design, also summarized in Table 3, has greatly inferior performance compared to the full outcome design in most of scenarios. In some scenarios, the reduced outcome design performs poorly because it completely ignores periodic efficacy evaluations and does not model time to death separately. Very often, the reduced outcome design fails to identify doses that are unacceptable due to inefficacy or death, as shown in Scenarios 3 and 4. When all doses have unacceptably high PD probability, in Scenario 4, only 21% of the trials were stopped early by the reduced outcome design, so it clearly is unsafe. For Scenario 8, where d_1 and d_2 have high probabilities of PD, the reduced outcome design declares these doses unacceptable less often, 50% vs 82% for d_1 and 34% vs 38% for d_2 compared with the full outcome designs. In Scenario 1, $p_{\text{D}}^{\text{true}}$ decrease significantly, while $p_{\text{PD}}^{\text{true}}$ does not, and dose 1 is truly optimal. Because the reduced outcome design combines death and PD, it selects the true optimal dose only 53% of the time compared to 77% under the full outcome model. A similar difference is seen in Scenario 2, where the truly optimal doses are selected 93% vs 64% of the time by the full vs reduced outcome designs. Scenarios 1 and 2 show that combining the terminal event death with the nonterminal event PD often results in much poorer dose selection. In Scenarios 5-10, the reduced outcome design identifies the true optimal doses much less often, for example, 25% vs 60% and 83% and 91% under the reduced vs full outcome designs in Scenarios 7 and 8, respectively. In Scenario 8, while PD occurrence decreases from 0.60 to 0.39 with doses 3 and 4, the expected occurrences of CR, $\overline{\pi}_{\bullet 3}$ increase sharply from 0.38 to 0.80 (shown in Table 3 and Supplementary Table 3). Since the full outcome design uses the ordinal response outcomes, it correctly identifies dose 4 as optimal much more often than the reduced outcome design. Figures 3A and 4A plot the differences between the two designs, $p_m^{\text{unacc}}(\text{Full}) - p_m^{\text{unacc}}(\text{Reduced})$ for safety and $p_m^{\text{sel}}(\text{Full}) - p_m^{\text{sel}}(\text{Reduced})$ for reliability, with positive differences corresponding to better performance by the full outcome design.

To examine how much the full outcome design's performance is improved by using a larger sample size, we reran the simulations using $N_{\max} = 120$. Supplementary Table 5 summarizes the results under all scenarios, showing that the performance is greatly improved in most scenarios. Figures 3B and 4B compare the performance metrics of the designs with $N_{\max} = 60$ and 120, in terms of the differences $p_m^{\text{unacc}}(\text{N} = 120, \text{Full}) - p_m^{\text{unacc}}(\text{N} = 60, \text{Full})$ and $p_m^{\text{sel}}(\text{N} = 120, \text{Full}) - p_m^{\text{sel}}(\text{N} = 60, \text{Full})$. Positive differences for truly unacceptable doses and truly optimal doses indicate superior performance with the larger sample size. Identification of truly unacceptable doses also is improved by larger N for all scenarios, except the one case of dose 4 in Scenario 5 whose true death probability equals its threshold. Dose selection also is noticeably improved by larger $N_{\max}$, especially in Scenarios 1, 4, and 7.

5 | DISCUSSION

We have presented a phase I-II clinical trial design that monitors dose acceptability and selects the optimal dose based on a vector of complex discrete and continuous outcomes that correspond to the way that patient outcomes actually are monitored in many trials. The design is motivated by a trial of a targeted agent combined with immunotherapy for treating

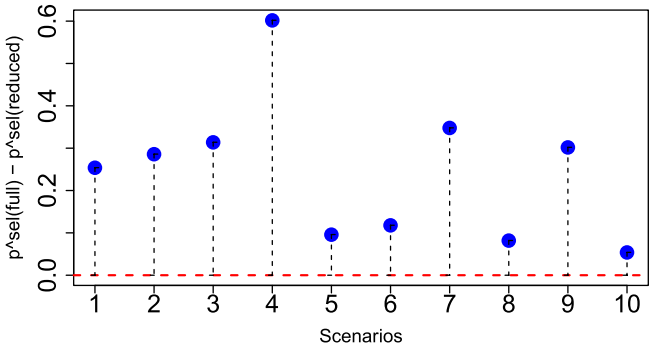

(A) Full vs Reduced Designs

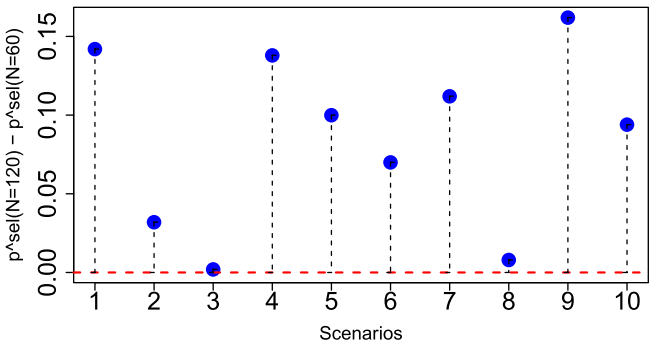

(B) $N_{\max} = 60$ vs 120

FIGURE 4 [Comparison of true optimal dose selection probabilities] Plots of, A, $p_m^{\text{sel}}(\text{Full, N} = 60) - p_m^{\text{sel}}(\text{Reduced, N} = 60)$ and, B, $p_m^{\text{sel}}(\text{Full, N} = 120) - p_m^{\text{sel}}(\text{Full, N} = 60)$. Larger positive values correspond to superior performance in true optimal dose selection by the full versus reduced outcome designs, both with 60 patients in (A), and of maximum sample size 120 versus 60 patients for the full outcome design in (B) [Colour figure can be viewed at wileyonlinelibrary.com]

metastatic renal cell cancer. A finite partition of the nonfatal outcome combination is defined to facilitate utility elicitation. In the application, $(\boldsymbol{Y}, \boldsymbol{Z})$ was mapped to a 33 set partition, which is sufficiently granular to represent $(\boldsymbol{Y}, \boldsymbol{Z})$ with little loss of information but still simple enough to allow utilities to be elicited. While the subjectivity of the utilities may be questioned, we consider this to be a strength of our methodology, rather than a weakness. Given the partition, the utilities provide an explicit quantification of the desirability of the possible outcomes, that is, the basis for choosing doses. In contrast, while all statistical methods require subjective decisions for their implementation, the underlying utilities often are not made explicit. For example, in conventional hypothesis testing, the common practice of specifying Type I error probability 0.05 and Type II error probability 0.20 implies that a false positive error is four times as important as a false negative error at the specified targeted alternative parameter. This is a highly subjective assumption that may not be appropriate in many settings. In practice, this implicit weighting of the importance of these two types of error, and the choice of the alternative parameter value, seldom are questioned. Thus, in general, since all decision-making relies on subjective criteria, we feel that making the actual criteria explicit is preferable to not doing so. While the design was motivated by a phase I/II trial in clear cell renal cell carcinoma, the practice of evaluating solid tumors as a categorical variable by scheduled imaging while also continuously monitoring signs/symptoms of progression that trigger unscheduled is extremely common in oncology. A closely related emerging practice is the use of wearable devices and smartphones to continuously monitor a patient's signs and symptoms, as well as treatment efficacy and toxicity.

Our simulations show that the design performs well under a wide variety of dose-outcome scenarios, and that incorporating the actual observational processes in a trial is very useful for making correct decisions with high probability, as shown by comparison to a simplified version of the design using two reduced outcomes. Simulations of the design with a larger sample size indicate that the performance of phase I-II designs for trials with complex outcomes can be improved greatly by increasing $N_{\max}$.

ACKNOWLEDGEMENTS

The research of Juhee Lee was supported by NSF grant DMS-1662427 and NOAA-ECOHAB PROGRAM (Grant No. NA17NOS4780183, ECOHAB #905). Pavlos Msaouel was supported by a Conquer Cancer Foundation Young Investigator Award and by a Kidney Cancer Association Young Investigator Award.

ORCID

Juhee Lee https://orcid.org/0000-0002-9787-3830

REFERENCES

1. Motzer RJ, Escudier B, McDermott DF, et al. Nivolumab versus everolimus in advanced renal-cell carcinoma. *New England J Med*. 2015;373:1803-1813.
2. Du W, Huang H, Sorrelle N, Brekken RA. Sitravatinib potentiates immune checkpoint blockade in refractory cancer models. *JCI Insight*. 2018;3:Advance Online Publication. https://doi.org/10.1172/jci.insight124184.
3. Eisenhauer EA, Therasse P, Bogaerts J, et al. New response evaluation criteria in solid tumours: revised RECIST guideline (version 1.1). *Eur J Cancer*. 2009;45(2):228-247.
4. Braun TM. The bivariate continual reassessment method: extending the CRM to phase I trials of two competing outcomes. *Control Clin Trials*. 2002;23:240-256.
5. Thall PF, Cook JD. Dose-finding based on efficacy–toxicity trade-offs. *Biometrics*. 2004;60(3):684-693.
6. Yin G, Li Y, JY. Bayesian dose-finding in phase i/ii clinical trials using toxicity and efficacy odds ratios. *Biometrics*. 2006;62(3):777-787.
7. Mandrekar S, Qin R, Sargent D. Model-based phase I designs incorporating toxicity and efficacy for single and dual agent drug combinations: methods and challenges. *Stat Med*. 2010;29:1077-1083.
8. Yuan Y, Yin G. Bayesian phase I/II adaptively randomized oncology trials with combined drugs. *Ann Appl Stat*. 2011;5(2A):924.
9. Thall PF, Herrick RC, Nguyen HQ, Venier JJ, Norris JC. Using effective sample size for prior calibration in Bayesian phase I-II dose-finding. *Clin Trials*. 2014;11(6):657-666.
10. Guo B, Yuan Y. Bayesian phase I/II biomarker-based dose finding for precision medicine with molecularly targeted agents. *J Am Stat Assoc*. 2017;112(518):508-520.
11. Yuan Y, Yin G. Bayesian dose finding by jointly modelling toxicity and efficacy as time-to-event outcomes. *J Royal Stat Soc Ser C (Appl Stat)*. 2009;58(5):719-736.
12. Thall PF, Nguyen HQ, Braun TM, Qazilbash MH. Using joint utilities of the times to response and toxicity to adaptively optimize schedule–dose regimes. *Biometrics*. 2013;69(3):673-682.
13. Jin IH, Liu S, Thall PF, Yuan Y. Using data augmentation to facilitate conduct of phase I–II clinical trials with delayed outcomes. *J Am Stat Assoc*. 2014;109(506):525-536.
14. Zohar S, Chevret S. Recent developments in adaptive designs for phase I/II dose-finding studies. *J Biopharm Stat*. 2007;17(6):1071-1083.
15. Yuan Y, Nguyen HQ, Thall PF. *Bayesian Designs for Phase I–II Clinical Trials*. New York, NY: Chapman & Hall/CRC; 2016.
16. Yan F, Thall PF, Lu KH, Gilbert MR, Yuan Y. Phase I-II clinical trial design: a state-of-the-art paradigm for dose finding with novel agents. *Ann Oncol*. 2018;29:694-699.
17. Lee J, Thall PF, Rezvani K. Optimizing natural killer cell doses for heterogeneous cancer patients on the basis of multiple event times. *J Royal Stat Soc Ser C (Appl Stat)*. 2019;68:461-474.
18. Gorfine M, Hsu L. Frailty-based competing risks model for multivariate survival data. *Biometrics*. 2011;67(2):415-426.
19. Lee KH, Dominici F, Schrag D, Haneuse S. Hierarchical models for semicompeting risks data with application to quality of end-of-life care for pancreatic cancer. *J Am Stat Assoc*. 2016;111(515):1075-1095.
20. Fine JP, Jiang H, Chappell R. On semi-competing risks data. *Biometrika*. 2001;88(4):907-919.
21. Ashford JR, Sowden RD. Multivariate probit analysis. *Biometrics*. 1970;26:535-546.
22. Chib S, Greenberg E. Analysis of ultivariate probit models. *Biometrika*. 1998;85:347-361.
23. Lagarde F, Beausoleil C, Blecher SM, et al. Non-monotonic dose-response relationships and endocrine disruptors: a qualitative method of assessment. *Env Health*. 2015;14:1-15.
24. Ursino M, Gasparini M. A new parsimonious model for ordinal longitudinal data with application to subjective evaluations of a gastrointestinal disease. *Stat Methods Med Res*. 2018;27(5):1376-1393.
25. Piccolo D, Simone R, Iannario M. Cumulative and CUB models for rating data: a comparative analysis. *Int Stat Rev*. 2019;87(2):207-236.
26. Wellhagen GJ, Kjellsson MC, Karlsson MO. A bounded integer model for rating and composite scale data. *AAPS J*. 2019;21(4):74.
27. Ibrahim JG, Chen M-H, Sinha D. Bayesian survival analysis. *Wiley StatsRef Stat Ref Online*. 2014.
28. Thall PF, Nguyen HQ. Adaptive randomization to improve utility-based dose-finding with bivariate ordinal outcomes. *J Biopharm Stat*. 2012;22(4):785-801.
29. Yan D, Wages N, Dressler E. Improved adaptive randomization strategies for a seamless Phase I/II dose-finding design. *J Biopharm Stat*. 2019;29(2):333-347.
30. Chapple AG, Thall PF. A hybrid phase I-II/III clinical trial design allowing dose re-optimization in phase III. *Biometrics*. 2019;75(2):371-381.

SUPPORTING INFORMATION

Additional supporting information may be found online in the Supporting Information section at the end of this article.

How to cite this article: Lee J, Thall PF, Msaouel P. A phase I-II design based on periodic and continuous monitoring of disease status and the times to toxicity and death. *Statistics in Medicine*. 2020;39:2035–2050. https://doi.org/10.1002/sim.8528